DUAL FREQUENCY DIFFERENTIAL IMPEDANCE TOMOGRAPHY - PHANTOM STUDIES

A.Bujnowski* and J.Wtorek*

* Gdańsk University of Technology/Department of Biomedical Engineering, Gdańsk, Poland

bujnows@biomed.eti.pg.gda.pl

Abstract: Electrical Impedance Tomography (EIT) is an imaging technique that produces images of electrical properties of measured object. There exist variety of systems and measurement techniques. A modified version of EIT, thus also a strategy of measurement is presented in this paper. A voltage excitation signal contains sum of two sinusoidal waveforms of different frequency. However, the resulting signal is proportional to a difference of two associated currents. The results from phantom measurements are presented.

Introduction

The measurement system is PC–based, differential dual frequency EIT system developed at the Biomedical Engineering Department, Gdańsk University of Technology [1]. The signal applied to the examined object is a sum of two sinusoids (Eq. 1):

$$U_e = \sum_{n=1,2} A_n \sin(\omega_n t + \varphi_n) \qquad (1)$$

The measured resulting signal can be in the form of a sum or a difference of currents associated with each particular excitation sinusoid. As the object is described by complex conductivity only real or imaginary part is processed at a given time.

To minimize quantisation error a demodulation and subtraction is performed by analogue method. The quality of obtained images depends on quality of measurement system and reconstruction algorithm used. Results from phantom studies are presented in the paper. Data are collected using voltage to current strategy of measurement. Two methods of image reconstruction have been used: a backprojection and a one-step Gauss-Newton algorithms.

Methods

The measurement set-up consists of dual frequency EIT system. It has a distributed architecture containing so-called active electrodes (AE) [1]. The term AE stands for an electronic measurement and processing circuit combined with two-parts Ag/AgCl electrode (i.e. compound electrode). The electronic boards are directly attached to the Ag/AgCl electrodes. AE can be configured as voltage to current or current to voltage circuit. A shallow circular tank made of perspex, 172 mm in diameter and 20 mm in height, is used. At the boundary of the tank 16 AEs are placed. Tank is filled with KCl solution having concentration equal to 0.4 mol. As a perturbation a piece of fresh cucumber is used. Also other materials, however non-dispersive, brass, aluminum and Perspex are used. The cucumber has a similar conductivity to the surrounding solution, while other perturbation, i.e. metal and Perspex, are very contrastive.

Two types of reconstruction algorithms have been developed, backprojection and Gauss-Newton one. The current-mode backprojection algorithm is fast and used mainly for a rapid validation of measurement data [2]. It is implemented directly in measuring hardware and it takes only a few second to obtain the reconstructed image. The measurement data are stored in ASCII file formatted compatible to the Maltab m-file. Data can be transferred to the external fast computer to perform reconstruction using other algorithms, e.g. Gauss-Newton or the sensitivity matrix-based one [3].

It is important to know, at this stage of experiments, the dependency of the object complex conductivity versus frequency for dual frequency measurements. Knowledge of the complex conductivity vs. frequency is necessary to enable proper selection of excitation signal frequency.

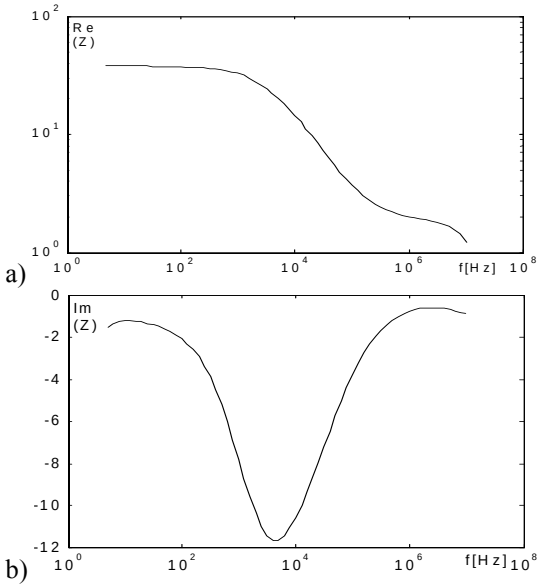

Figure 1: Real and imaginary part of impedance vs. frequency of the cucumber sample measured using the Solartron SI1260

ISSN: 1727-1983

The piece of cucumber has been measured using a specially developed cell and Solartron SI1260 impedance analyzer before performing tomographic measurements. The results of the measurements show a strong dispersive property of the cucumber (figure 1). It can be seen that the maximum value of imaginary part, thus also a maximal phase shift, occurs for the frequency of several tens of kilohertz (figure 1b). Thus, the biggest value of resistivity difference is obtained for frequency markedly below and above this frequency. In contrary to that figure 2 is showing the frequency dependent complex impedance of the KCl solution used for filling the tank. It exhibits no dispersion in the considered range of frequency. Small deviations of the imaginary and real part from the theoretical values for a very low frequency are caused by the presence of large electrode impedance. The deviations at high frequency are mainly involved by limited bandwidth of electronic interface.

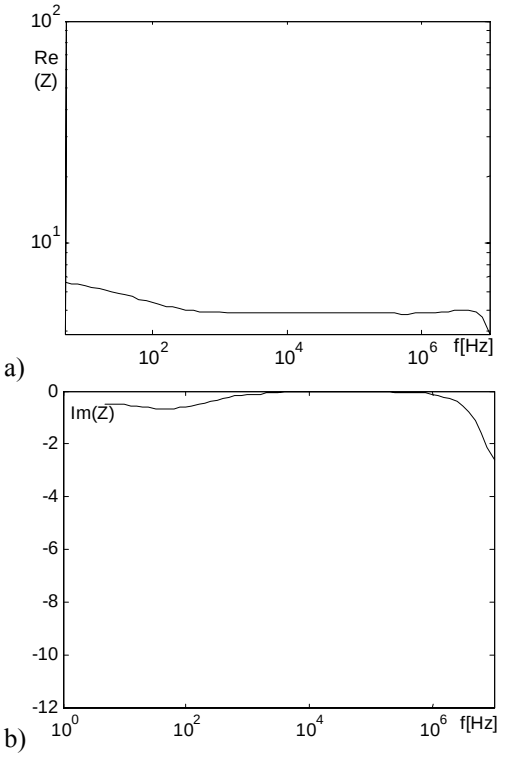

Figure 2: Real and imaginary part of impedance vs. frequency of KCl solution measured using Solartron

Reconstructions have been performed using the Gauss-Newton algorithm:

$$\Delta\boldsymbol{\sigma}^k = -\left\{\mathbf{J}^T\mathbf{J} + \left[\mathbf{J}'\right]^T\left[\mathbf{I}\otimes\mathbf{r}\right]\right\}^{-1}\mathbf{J}^T\mathbf{r} \qquad (2)$$

where $\Delta\boldsymbol{\sigma}^k$ – conductivity correction for i[th] iteration, $\otimes$ – Kronecker product, $\mathbf{J}$ – Jacobian with entries defined as $J_{ij} = \partial i_i^o / \partial\sigma_j$, $\mathbf{J}'$ – the derivative of Jacobian with respect to conductivity, $\mathbf{I}$ – unit matrix, and residuum $\mathbf{r} = \mathbf{i}^o\left(\boldsymbol{\sigma}^k\right) - \mathbf{i}^m$.

Calculation of the Hessian is time-consuming and difficult. However, a close inspection of the relation reveals that the second part of the Hessian contains multiplication of the unit matrix and residuum. In the event of the residuum containing small values, this product can be omitted. However, in the considered case the measured difference signal is really a small one. Thus the second term in bracket can be omitted. The final form of the relation used in the reconstruction is:

$$\boldsymbol{\sigma} = \boldsymbol{\sigma}_0 - \left[\mathbf{J}^T\mathbf{J} + \lambda\cdot diag\left(\mathbf{J}^T\mathbf{J}\right)\right]^{-1}\mathbf{J}^T\mathbf{r}\,, \qquad (3)$$

where λ is a regularisation co-efficient, calculated for an ill-conditioned problem. It can be evaluated using appropriate procedures. In our study by using diagonal matrix $diag(\mathbf{J}^T\mathbf{J})$ a constant value of λ was assumed. Jacobian is calculated using the following formula:

$$\frac{\partial i_{ei}}{\partial\sigma_j} = \int_{S_{el}} \frac{1}{z_{ei}}\mathbf{Y}_i^{-1}\frac{\partial\mathbf{Y}_i}{\partial\sigma_j}\mathbf{V}\,d\mathbf{S}\,, \qquad (3)$$

where $\mathbf{Y}_i$ – the admittance matrix for i^{th} projection; S_{el} – electrode surface, σ_j – conductivity of j^{th} element of the object, z_{ei} – characteristic impedance of the i^{th} electrode.
FE mesh used in inverse problem is presented in Fig. 3. Number of elements is equal to number of independent measurement.

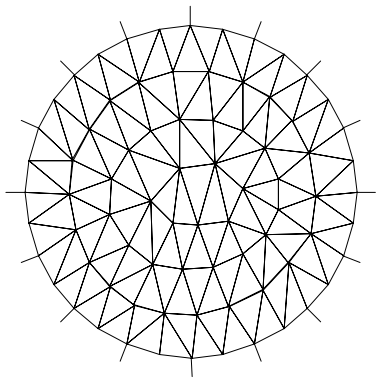

Figure 3: The FE mesh used for data reconstruction.
The piece of cucumber has been immersed in a solution of KCl.

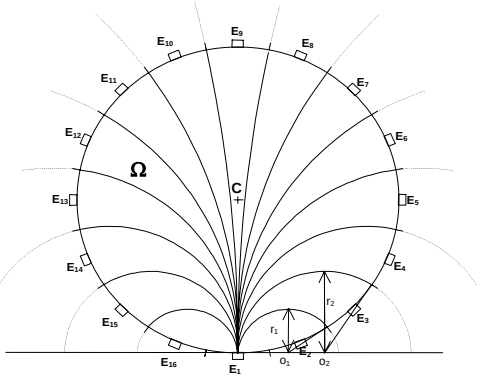

Figure 4: The predicted path of current flow in the current-mode backprojection.

ISSN: 1727-1983

The current-mode backprojection algorithm is using predicted path of the current flowing from voltage injecting to all current receiving electrodes. The predicted current paths are calculated according to formula (4).

$$\begin{cases} x_l = \dfrac{R*\cos(\alpha_l + \alpha_B)}{\cos(\alpha_l)} \\ y_l = \dfrac{R*\sin(\alpha_l + \alpha_B)}{\cos(\alpha_l)} \\ r_l = R*tan(\alpha\ ) \end{cases} \qquad (4)$$

l=-(N-1),-(N-3),...1,3,..N-1

$$\alpha = \frac{n*\beta}{2} \qquad \beta = \frac{\pi}{N}$$

where: N – number of electrodes, R – radius of the object.

The resulting domain subdivision is shown in figure 4. For N-electrode system it is necessary to prepare N of such images for each projection. To produce KxK output image Kx(K*N) integer **S** matrix is generated The matrix **S** is subdivided for H_{nk} regions where the n index describes the current receiving electrode and the k index is corresponding to the projection Colours of the matrix elements are assigned to the current receiving electrode index. The reconstruction process for each measurement projection assigns the differential result from k-th measuring electrode to the H_{nk} area. All pixels values of the output image belonging to the H_{nk} are incremented by value I_{nk} (current measured at the k-th electrode while voltage has been applied to the n-th one) number.

After all projections output image pixels contain the sum of the currents for each projections. By dividing each pixel by N and assuming that conductivity of the region H_{nk} is proportional to the ΔI_{nk} ($\Delta I_{nk} = I_{nkf1} - I_{nkf2}$), the image of average difference in the conductivity distribution within the object is given:

$$\Delta\sigma_{H(n,k)} = K(\Delta I_{nk}) \qquad (5)$$

The frequency of the excitation signal components have been selected correspondingly f_1=10 kHz and f_2=10 MHz according to spectroscopic data collected from samples of cucumber and saline samples.

Results

Averaged values of data from differential measurements for homogenous object are shown in figure 5. Theoretically, measurements for all channels should be exactly the same. It is easy way to detect the differences in measurement channels.

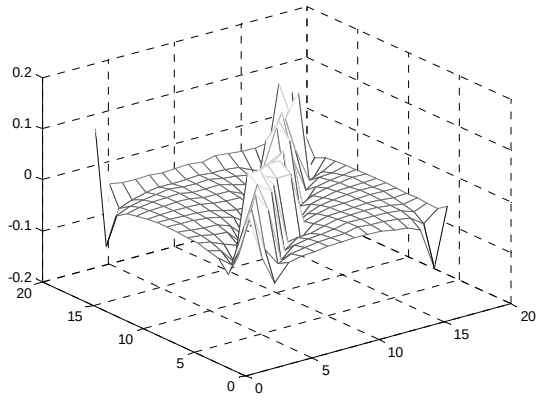

Figure 5: Mean value of the series of the measurement for phantom.

Instability of measurement can be also achieved by calculation of variance for each channel (Fig. 6).

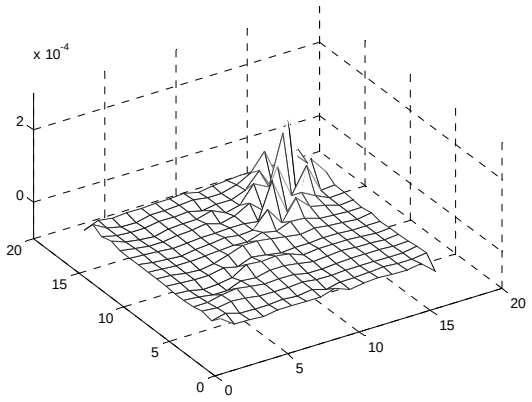

Figure 6: Variation of the series of the measurements. One unstable electrode causes the rise of variation around it.

Results of differential reconstruction using the backprojection algorithm for different location of cucumber are presented in the figure 7. The figure presents the photograph of the perturbation on the left and results of backprojection algorithm on the right side. These images have been obtained for reconstruction basing on real part of data.

The same date have been used for reconstruction using Gauss-Newton algorithm (Fig. 8). Only images are presented.

ISSN: 1727-1983

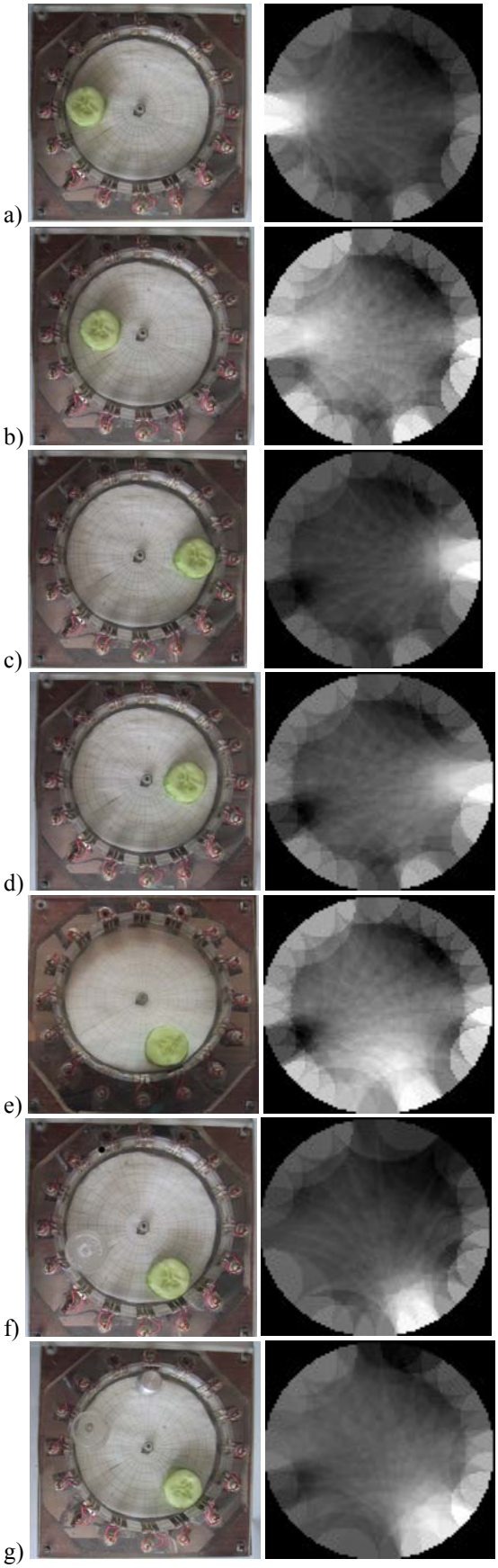

Figure 7: A set of examples of phantom data reconstruction for differential measurements at two frequency: f_2=10kHz, f_1=1MHz

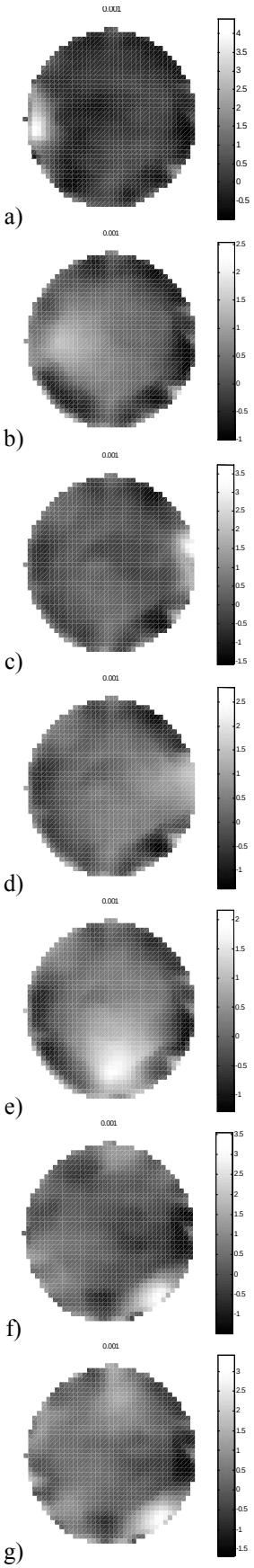

Figure 8: A reconstruction of the corresponding data using single-step reconstruction algorithm. Due to

ISSN: 1727-1983

different enumeration of the boundary nodes produced figures are rotated 90 degrees counterclockwise.
Imaginary part of data has been also performed (Fig. 9).

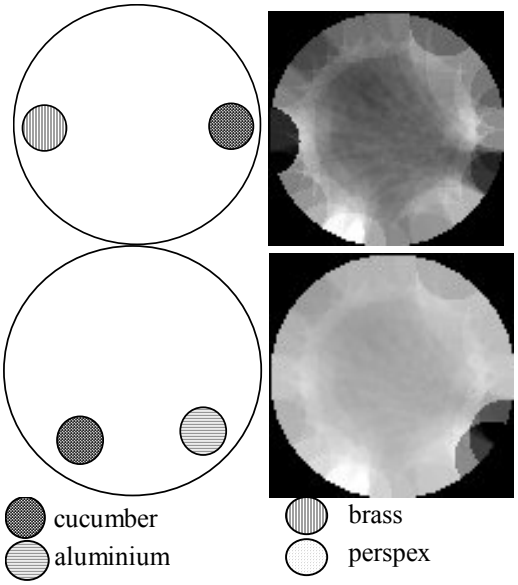

Figure 9: Example of reconstruction for imaginary part of signal

More different perturbations are used. Aside cucumber cylinders made of brass, aluminium and perspex are also used.

Discussion

Result of measurement for single or dual frequency is a symmetrical matrix (N×N N-electrodes total) containing the currents that are flowing between the electrodes. The typical reconstruction algorithm demands input data in the form of a residual vector that is calculated as difference between, mainly sequential, measurements of perturbed and homogenous objects. However, the latter are usually obtained using FEM simulation. Input data from dual-frequency simultaneous and differential measurement already contain residual values so the error, which comes from discrepancy between FEM model and the object is essentially reduced and can be omitted.
The dual frequency imaging technique requires more careful calibration of the measurement system than the single frequency one. It is due to increased number of system components that can introduce errors. However, differential measurement technique has some advantages over the single frequency one. For distributed-architecture systems, like the one presented in the paper, a very important factor is precise calibration of each active electrode. The AE's should process the signal exactly with the same accuracy. Moreover, this should obey for the whole frequency bandwidth of the system. The one-time calibration should be performed for each electrode by applying the known signal and measuring the response.

The electrode polarization impedance strongly depends on frequency of applied current or voltage. An influence of this effect on quality of images may be reduced using current to voltage strategy of measurement. Otherwise, a precise correction should be included in the system. It has not been done yet in our systems. It is easy to notice this influence in reconstructed images as ring-shaped image distortion.

Conclusions

A two-frequency differential system has been developed. Examples of reconstructed images for real and imaginary part have been obtained. However, the images obtained are corrupted by relatively high level of noise.

References

[1] BUJNOWSKI A., WTOREK, J. and NOWAKOWSKI A. (2001): 'A versatile dual frequency electroimpedance tomograph', Proc of XI International Conference on Electrical Bioimpedance, Oslo, Norway, 2001, pp.505-509
[2] BUJNOWSKI A. and WTOREK J. (2004): 'Backprojection Algorithm for Current mode EIT', *Proc of XII International Conference on Electrical Bioimpedance & V Electrical Impedance Tomography*, Gdańsk, Poland, 2004, pp.595-598
[3] WTOREK J. and BUJNOWSKI A. (2001): 'A reconstruction algorithm based on current measurements and the knowledge of electrode impedance', *Proc of XI International Conference on Electrical Bioimpedance*, Oslo, Norway, 2001, pp. 501-504

ISSN: 1727-1983